# Poly(oxyethylene)−Water Interactions: A Molecular Dynamics Study

**Kenzabu Tasaki**[†]

*Contribution from the Department of Chemistry, Washington University, Campus Box 1134, St. Louis, Missouri 63130*

*Received March 28, 1995. Revised Manuscript Received May 6, 1996*[⊗]

**Abstract:** Molecular dynamics simulations of a poly(oxyethylene) (POE) chain with 15 ethylene oxide (EO) units have been performed in an aqueous solution for 2 ns at 300 K and for 1 ns at 373 K, a cloud point for POE. The conformation and the hydration structure of POE and the structure and the dynamics of water molecules in the vicinity of POE were examined. The conformation of POE was transformed from a collapsed chain in the gas phase to a helix in water which was maintained for 2 ns. After a simulated annealing at 1000 K, POE still showed a preference for a helix. An extended network of POE−water and water−water hydrogen bonds was found throughout inside the helix, stabilizing the helix backbone. The same helical conformation was maintained even at 373 K. The pair distribution functions for water oxygen atoms near POE indicated significantly enhanced water structures in the hydrophilic region of POE, and to a lesser extent in the hydrophobic region, at both 300 and 373 K. Considerably reduced translational movements of water molecules near POE were also observed at both temperatures. All the results obtained from the simulation are in good agreement with experiments. We discuss the solubility and the phase behavior of POE in water, based on the observation from the simulations.

## Introduction

The nature of water-soluble polymers in aqueous solutions is closely related to the interactions with water. In fact, the characteristics of some water-soluble polymers are very sensitive to the solvent.[1] Poly(oxyethylene) (POE),[2] $-[CH_2CH_2O]_n-$, is one of those polymers. Our NMR study of POE[4] demonstrated a significant conformational change in going from organic solvents to water, which is supported by various spectroscopic measurements.[5]

Our primary interest is two-fold: the POE's conformational behavior in water and the water structure in the vicinity of POE. We discuss these issues in relation to the solubility and the phase behavior of POE in water. POE has a unique solubility in that POE dissolves in water to any extent. This characteristic stands in sharp contrast to water solubility of other polyethers such as poly(oxypropylene), $-[CH_2CH(CH_3)O]_n-$, and poly(oxytrimethylene), $-[CH_2CH_2CH_2O]_n-$, insoluble in water with different degrees of hydrophobicity. It is thus of significant interest to examine the interactions of both hydrophilic and hydrophobic groups of polyethers with water in order to understand the function of each group in the miscibility of polyethers in water. Also the subjects of our report are the role of water in solvation of a polyether and the relationship between the solubility and the conformation in water. It is still not clear to what extent the hydrophobic groups and the conformations of water-soluble polymers contribute to their solubilities, despite intensive solubility studies of polymers such as POE.[6] Yet, it is experimentally difficult to separate these contributions. In this report, we take POE as our first model for the functionality of the conformation and the hydrophilic and the hydrophobic groups in the solubilities of polyethers.

Recently, among many other applications, POE has been increasingly used in biomedical applications such as separation of biological materials.[7] These biological functions of POE are due largely to its ability to control the solubilities and the molecular dimensions of other biological molecules including POE itself in aqueous solutions. There is also significant interest in the hydration of POE in surfactant chemistry as well since

[†] Present address: Mitsubishi Chemical America, 99 W Tasman Dr., Suite 200, San Jose, CA 95134.

[⊗] Abstract published in *Advance ACS Abstracts,* August 1, 1996.

(1) Molyneux, P. *Water-Soluble Synthetic Polymers: Properties and Behavior*; CRC Press: Boca Raton, 1983; Vol. 1, p 19.

(2) According to J. M. Harris, poly(ethylene glycol) refers to polyols with molecular weight <20 000, poly(ethylene oxide) refers to higher molecular weight polymers, and poly(oxyethylene) is not specific in this regard.[3] Since our system in this study does not necessarily model high molecular weight polymers, we have chosen the name poly(oxyethylene).

(3) Harris, J. M. In *Poly(ethylene glycol) Chemistry*; Harris, J. M., Ed.; Plenum: New York, 1992; pp 1.

(4) Tasaki, K.; Abe, A. *Polym. J.* **1985**, *17*, 641.

(5) (a) Koenig, J. L.; Angood, A. C. *J. Polym. Sci.* **1970**, *8*, 1787. (b) Liu, K.-J.; Parsons, J. L. *Macromolecules* **1969**, *2*, 529. (c) Matsuura, H.; Fukuhara, K. *J. Mol. Struct.* **1985**, *126*, 251. (d) Maxfield, J.; Shepherd, I. W. *Polymer* **1975**, *16*, 505.

(6) (a) Bailey, F. E., Jr.; Callard, R. W. *J. Appl. Polym. Sci.* **1959**, *1*, 56. (b) Bailey, F. E., Jr.; Callard, R. W. *J. Appl. Polym. Sci.* **1959**, *1*, 373. (c) Saeki, S.; Kuwahara, N.; Nakata, M.; Kaneko, M. *Polymer* **1976**, *17*, 685. (d) Malcolm, G. N.; Rowlinson, J. S. *Trans. Faraday Soc.* **1957**, *53*, 921. (e) Nakayama, H. *Bull. Chem. Soc. Jpn.* **1970**, *43*, 1683. (f) Powell, G. M.; Bailey, F. E. In *Kirk-othmer Encyclopedia of Chemical Technology, Second Supplement*; Sranden, A., Ed.; Interscience: New York, 1960; pp 597. (g) Bailey, F. E., Jr.; Koleske, J. V. *Polyethylene Oxide*; Academic Press: New York, 1976.

(7) (a) Abuchowski, A.; Kazo, G. M.; Verhoest, C. R., Jr.; Van Es, T.; Kafkewitz, D.; Nucci, M. L.; Viau, A. T.; Davis, F. F. *Cancer Biochem. Biophys.* **1984**, *7*, 175. (b) Albertsson, P.-Å. *Partition of Cell Particles and Macromolecules*; Wiley: New York, 1986. (c) Herschfield, M. S.; Buckley, R. H.; Greenburg, M. L.; Melton, A. L.; Schiff, R.; Hatem, C.; Kurtzberg, J.; Markert, M. L.; Kobayashi, R. H.; Kobayashi, A. L.; Abuchowski, A. *New Eng. J. Med.* **1987**, *316*, 589. (d) Beckman, J. S.; Minor, R. L.; White, C. W.; Repine, J. E.; Rose, G. M.; Freeman, B. A. *J. Biol. Chem.* **1988**, *263*, 6884. (e) Inada, Y.; Matsushima, A.; Kodera, Y.; Nishimura, H. *J. Bioact. Compat. Polym.* **1990**, *5*, 343. (f) *Poly(Ethylene Glycol) Chemistry*; Harris, J. M., Ed.; Plenum: New York, 1992.

(8) Nilsson, P.-G.; Wennerström, H.; Lindman, B. *J. Phys. Chem.* **1983**, *87*, 1377.

(9) (a) Attwood, D. *J. Phys. Chem.* **1968**, *72*, 339. (b) El Eini, D. I. D.; Barry, B. W.; Rhodes, C. T. *J. Colloid. Interface Sci.* **1976**, *54*, 348. (c) Elworthy, P. H.; Macfarlane, C. B. *J. Chem. Soc.* **1962**, 537. (d) Corkill, J. M.; Goodman, J. F.; Wyer, J. *Trans. Faraday Soc.* **1969**, *65*, 9. (e) Schott, H. *J. Colloid Interface Sci.* **1967**, *24*, 193. (f) Schott, H. *J. Pharm. Sci.* **1969**, *58*, 1521. (g) Arnarson, T.; Elworthy, P. H. *J. Pharm. Pharmacol.* **1981**, *33*, 141. (h) Mitchell, D. J.; Tiddy, G. J. T.; Waring, L. *J. Chem. Soc., Faraday Trans.* **1983**, *79*, 975. (i) Podo, F.; Ray, A.; Némethy, G. *J. Am. Chem. Soc.* **1973**, *95*, 6164.

S0002-7863(95)01005-5 CCC: $12.00 

the hydration structure is closely related to the phase behavior and the size of the micelles.[8] A number of investigations on the hydration of POE micelles have been reported.[9]

The structural and the thermodynamic properties of POE in water have been extensively examined.[4−18] Yet many characteristics of POE in water are either only qualitatively understood or still controversial. For example, experimental reports have shown that the C−C bond rotation predominantly prefers the gauche state over trans in aqueous solutions.[4,5] Nonetheless, the interpretations have been mixed.[10−12] The conformation of POE in aqueous solutions previously reported ranges from a random coil[5a,d,13,14] to a helix.[5b,c] Molecular dynamics (MD) simulations provide insight into the local conformation as well as the hydration of a polymer in water at the atomic level. Though detailed analyses of the solvation of peptides or carbohydrates in water have been carried out by MD simulations,[19,20] very few studies have been reported for atomic interactions of industrially important water-soluble polymers with water.

Equilibration of the conformation for a chain molecule requires in general an extensively long simulation time in a condensed phase. The relaxation times for low-frequency motions of even low molecular-weight polymers are in the order of microseconds or more.[21] It is thus often difficult to determine a stable conformation for a polymer chain in water by a computer simulation within a reasonable CPU time. Here, we employed a combination of several techniques to examine the stability of the POE conformation in water: a 2-ns simulation at room temperature, the temperature dependence of the conformation at a higher temperature, a simulated annealing at 1000 K, and changing the solvent to an organic solvent and then back to water. A number of computer simulations of POE have been performed in various states.[22] Among them, short MD simulations of POE in an aqueous solution have been reported by Depner and co-workers[22a] and Gölander and co-workers.[22c] Depner et al.[22a] performed a simulation for a similar size POE chain as ours in water for 100 ps, and only 20-ps simulation was carried out in Gölander's work.[22c] No detailed interactions of POE with water were reported in either study.

Interactions between a water-soluble polymer and solvent molecules in solution are of primary importance in the determination of the structures of polymers. It has been found that while POE is flexible in nonpolar solvents, it becomes rather rigid in aqueous solution.[5a−c] From the enthalpic point of view, bridged hydrogen-bond models between water molecules and POE have been proposed to explain the strong gauche stability around the C−C bond.[10,15] However, the models are highly speculative. From the entropic point of view, little is known for the stability of the gauche conformation in aqueous solution, though several thermodynamics models have been presented.[11,12] Additionally, in the investigation of the POE hydration structure, determining the number of water molecules associated with an ethylene oxide (EO) unit has been one of the primary goals.[16] This number has been reported by various techniques.[5b,d,8,10,16−18] However, the reported numbers scatter over a wide range: 1,[17] 2,[10] 3,[5b,d,16,18] 4−5,[8] and 6[8] per EO unit.

Of interest also is the effect of a water-soluble polymer on its nearby water molecules. The entropy of mixing for POE and water is negative over nearly the whole composition range.[6d,11] If entropy loss in the excess free energy of solution arises from an increase in solvent "order" or "structure",[23] it is of considerable importance to understand the structure and the dynamics of water molecules in the vicinity of POE. It was found from ultrasonic absorption measurements[24] that the water structure near POE is altered. However, experimental work does not provide information with regard to the detailed molecular rearrangement of water in the vicinity of POE. In this report, we examine the structural and the dynamical aspects of water as a solvent. Particular emphasis is placed on how the structure of POE (or water) is altered by water (or by the proximity of POE).

Subsequently, we discuss the phase behavior of POE which exhibits an upper temperature limit of solubility,[6g,25] better known as a cloud point for its dilute solution. Its phase behavior has been a focus of numerous reports.[6−9,22c] A number of models have been proposed to explain the phase separation of POE in water. Kjellander and Florin[11] discussed the phase behavior of POE at a cloud point in terms of the enthalpy and the entropy changes of POE at a cloud point. Goldstein proposed a hydrogen bond model to explain the cloud point at which the hydrogen bonds between POE and water are presumably broken.[26] Samii and co-workers,[27] on the other hand, suggested that the phase separation results from the change in dipole−dipole interactions between POE and water which become less favorable for dissolution as temperature increases due to the conformational change of POE. We have performed an additional MD simulation of POE in water at 100 °C, a cloud point for POE, and have analyzed the solvent structure at that temperature and compared with that observed at room temperature. We examine the above models, based on the results from our MD simulations.

## Molecular Dynamics Simulations

**Force Field.** The potential energy function used in the MD simulations in this study was of the following type:[28]

(10) Matsuura, H.; Fukuhara, K. *Bull. Chem. Soc. Jpn.* **1986**, *59*, 763.
(11) Kjellander, R.; Florin, E. *J. Chem. Soc., Faraday Trans. 1* **1981**, *77*, 2053.
(12) Blandamer, M. J.; Fox, M. F.; Powell, E.; Stafford, J. W. *Makromol. Chem.* **1969**, *124*, 222.
(13) (a) Hawley, S. A.; Dunn, F. *J. Chem. Phys.* **1969**, *50*, 3523. (b) Hawley, S. A.; Kessler, L. W.; Dunn, F. *J. Acoust. Soc. Am.* **1965**, *38*, 521. (c) Kessler, L. W.; O'Brien, W. D.; Dunn, F. *J. Phys. Chem.* **1970**, *74*, 4096.
(14) Braun, D.; Törmälä, P. *Makromol. Chem.* **1978**, *179*, 1025.
(15) (a) Horne, R. A.; Almeida, J. P.; Day, A. F.; Yu, N.-T. *J. Colloid Interface Sci.* **1971**, *35*, 77. (b) Luck, W. *Fortschr. Chem. Forsch.* **1964**, *4*, 653.
(16) Antonsen, K. P.; Hoffman, A. S. In *Poly(Ethylene Glycol) Chemistry*; Harris, J. M., Ed.; Plenum: New York, 1992; p 15.
(17) Maconnachie, A.; Vasudevan, P.; Allen, G. *Polymer* **1978**, *19*, 33.
(18) Rösch, M. *Kolloid-Z.* **1956**, *147*, 78.
(19) (a) Rossky, P. J.; Karplus, M. *J. Am. Chem. Soc.* **1979**, *101*, 1913. (b) Rossky, P. J.; Karplus, M.; Rahman, A. *Biopolymers* **1979**, *18*, 825. (c) van Gunsteren, W. F.; Berendsen, H. J. C. *J. Mol. Biol.* **1984**, *176*, 559.
(20) (a) Brady, J. W. *J. Am. Chem. Soc.* **1989**, *111*, 5155. (b) Ha, S.; Gao, J.; Tidor, B.; Brady, J. W.; Karplus, M. *J. Am. Chem. Soc.* **1991**, *113*, 1553.
(21) Ferry, J. D. *Viscoelastic Properties of Polymers*, 3rd ed.; Wiley: New York, 1980.
(22) (a) Depner, M.; Schürmann, B. L.; Auriemma, F. *Mol. Phys.* **1991**, *74*, 715. (b) Depner, M.; Schürmann, B. L. *J. Comp. Chem.* **1992**, *13*, 1210. (c) Gölander, C.-G.; Herron, J.; Lim, K.; Claesson, P.; Stenius, P.; Andrade, J. D. In *Poly(ethylene glycol) Chemistry*; Harris, J. M., Ed.; Plenum: New York, 1992; p 221. (d) Neyertz, S.; Brown, D.; Thomas, J. O. *J. Chem. Phys.* **1994**, *101*, 10064. (e) Müller-Plathe, F.; van Gunsteren, W. F. *J. Chem. Phys.* **1995**, *103*, 4745. (f) Neyertz, S.; Brown, D. *J. Chem. Phys.* **1995**, *102*, 9725.
(23) Franks, F. In *Water: A Comprehensive Treatise*; Frank, F., Ed.; Plenum: New York, 1973; Vol. 2, p 1.
(24) Hammes, G. G.; Lewis, T. B. *J. Phys. Chem.* **1966**, *70*, 1610.
(25) (a) Bluestone, S.; Mark, J. E.; Flory, P. J. *Macromolecules* **1974**, *7*, 325.30. (b) Bailey, F. E.; Powell, G. M.; Smith, K. L. *Ind. Eng. Chem.* **1958**, *50*, 8.
(26) Goldstein, R. E. *J. Chem. Phys.* **1984**, *80*, 5340.
(27) Samii, A. A.; Lindman, B.; Karlström, G. *Prog. Colloid, Polym. Sci.* **1990**, *82*, 1.
(28) Brooks, B. R.; Bruccoleri, R. E.; Olafson, B. D.; States, D. J.; Swaminathan, S.; Karplus, M. *J. Comp. Chem.* **1983**, *4*, 187.

$$V = \sum k_r(r - r_0)^2 + \sum k_\theta(\theta - \theta_0)^2 + \sum k_\phi\{1 + \cos(n\phi - \delta)\} + \sum 4\epsilon_{ij}\{(\sigma_{ij}/r_{ij})^{12} - (\sigma_{ij}/r_{ij})^6\} + \sum(q_i q_j/r_{ij}) \quad (1)$$

A number of force fields for POE have been proposed in the past.[22d,e,29] However, very few force fields were specifically parametrized for POE−water interactions. Here, we take the harmonic potential parameters and the van der Waals parameters from a previously developed force field[29b] and adjust the atomic charges and the torsion terms for aqueous-solution simulations of POE, using a model compound. Our intention is to gain a qualitative physical picture of POE in water without going through an extensive force field parametrization for a POE−water system. The force constants $k_r$'s and $k_\theta$'s for the stretching and the bending energies in eq 1 were directly taken from the force field developed for POE by Smith and co-workers[29b] except for the C−O−C bond. The harmonic potentials, $k_r$, $k_\theta$, $r_0$, and $\theta_0$, were derived from Hartree−Fock ab initio calculations.[29a] Our previous study, however, has shown that the bond angle C−O−C of 1,2-dimethoxyethane (1,2-DME), a low molecular weight homologue, optimized by MP2 gradient calculations[30] is 3° smaller than that optimized at the Hartree−Fock level.[31] We used the MP2 optimized geometries to fit the value of the standard angle $\theta_0$ in the second term of eq 1 for the bond angle C−O−C to be 108.0°. The Lennard-Jones parameters in eq 1 were determined so as to reproduce the potential well depths ($\epsilon_{ij}$) and the van der Waals radii ($2^{1/6}\sigma_{ij}$) of the atomic pair interaction potentials in the Smith et al.'s force field in which the Buckingham potential was used.[29b] For the gas-phase simulation, the same atomic charges as those proposed by Smith et al.[29b] were adopted for the electrostatic interactions, while the torsion terms were reparametrized by fitting to the MP2 ab initio calculations of 1,2-DME[30,31] due to the different torsion potential used in this study.[32] The atomic charges and the torsion parameters for the aqueous simulation are described below.

In the previous simulation of POE in aqueous solution,[22a] the hydrogen bond was not fully established between POE and water due to the small atomic charge for the POE ether oxygen, −0.3 e. The atomic charge for the ether oxygen atom in water has been augmented to −0.58 e due to polarization by water in Jorgensen's OPLS parameters.[33] This charge has been specifically parametrized for ether−water interactions.[33] We adopted the same value for the POE oxygen atomic charge in aqueous solution. For the hydrogen atom of POE, the same charge, 0.097 e, as that proposed by Smith et al.[29b] was used. The charge for the carbon atom was adjusted so as to neutralize a group $-CH_2-O-CH_2-$ or the terminal group $CH_3-O-CH_2$ used as a unit group for the nonbonded interaction treatment. As to the torsion terms, a number of MD simulations of 1,2-DME were performed in water. The torsion parameters were fitted to the conformational populations for the C−C and C−O bond rotations of 1,2-DME determined by NMR spectroscopy in $D_2O$.[4] Other force field parameters, the force constants and the Lennard-Jones parameters, were the same as those for the gas-phase simulation described above. Table 1 lists all the force field parameters used for both simulations, in the gas phase and water. The gauche populations for the C−C and the C−O bonds of 1,2-DME obtained from the simulation in water with the parameters listed in Table 1 were 0.86 and 0.08, respectively, in excellent agreement with the NMR result, 0.9 and 0.1, respectively.[4]

**Table 1.** Force Field Parameters Used in Molecular Dynamics Simulations in the Gas Phase and Aqueous Solution[a]

Stretching Parameters[b]

| bond | $r_0$, Å | $k_0$, kcal mol$^{-1}$ |
|---|---|---|
| C−C | 1.51 | 618.0 |
| C−H | 1.09 | 655.0 |
| O−C | 1.39 | 739.0 |

Bending Parameters[b]

| angle | $\theta_0$, deg | $k_\theta$, kcal mol$^{-1}$ | angle | $\theta_0$, deg | $k_\theta$, kcal mol$^{-1}$ |
|---|---|---|---|---|---|
| C−C−C | 111.05 | 107.0 | C−C−O | 109.09 | 172.0 |
| C−C−H | 109.54 | 86.0 | O−C−H | 110.17 | 112.0 |
| H−C−H | 108.36 | 77.0 | C−O−C | 108.00[c] | 149.0 |

Nonbonded Interaction Parameters[c]

| interacting pair | $4\epsilon_{ij}\{(\sigma_{ij}/r_{ij})^{12} - (\sigma_{ij}/r_{ij})^6\}$ | | interacting pair | $4\epsilon_{ij}\{(\sigma_{ij}/r_{ij})^{12} - (\sigma_{ij}/r_{ij})^6\}$ | |
|---|---|---|---|---|---|
| | $\epsilon_{ij}$, kcal mol$^{-1}$ | $\sigma_{ij}$, Å | | $\epsilon_{ij}$, kcal mol$^{-1}$ | $\sigma_{ij}$, Å |
| C···C | 0.095 | 3.44 | C···H | 0.031 | 3.23 |
| C···O | 0.138 | 3.15 | O···H | 0.044 | 2.93 |
| O···O | 0.199 | 2.85 | H···H | 0.098 | 3.00 |

Atomic Charges for Gas-Phase and Aqueous-Solution Simulations

| gas phase[b] | | aqueous solution[c] | |
|---|---|---|---|
| atom | charge | atom | charge |
| C | 0.066 | C | 0.096 |
| O | −0.256 | O | −0.580 |
| H | 0.097 | H | 0.097 |

Torsion Parameters[c]

| | gas phase | | | aqueous solution | | |
|---|---|---|---|---|---|---|
| torsion | $k_\phi$, kcal mol$^{-1}$ | $\delta$, deg | $n$ | $k_\phi$, kcal mol$^{-1}$ | $\delta$, deg | $n$ |
| CC−OC | −3.5 | 0.0 | 1 | −0.4 | 0.0 | 1 |
| CC−OC | 1.40 | 180.0 | 2 | −0.6 | 180.0 | 2 |
| CC−OC | 0.50 | 0.0 | 3 | 1.2 | 0.0 | 3 |
| OC−CO | | | | −3.8 | 0.0 | 1 |
| OC−CO | −1.35 | 180.0 | 2 | −1.7 | 180.0 | 2 |
| OC−CO | 0.60 | 0.0 | 3 | 0.8 | 0.0 | 3 |
| HC−OC[b] | 0.4 | 0.0 | 3 | 0.4 | 0.0 | 3 |

[a] The parameters were used for both gas-phase and aqueous-solution simulations unless mentioned otherwise. [b] Reference 27a. [c] Parametrized in this study.

**MD Simulation Protocol.** In the simulations, Newton's equations of motion were integrated numerically for every atom in the model system using the potential energy function described above. The POE chain studied here had the atomic composition of $C_{32}H_{66}O_{16}$ with 15 EO units.[34] The simulation was carried out under constant NVE conditions using the Verlet algorithm[36] with a time step of 1 fs. Initial velocities were selected from a Boltzmann distribution appropriate to the temperature. All atoms were treated individually, and all internal coordinates were relaxed during the simulation. Bond lengths involving hydrogen atoms in both solute and solvent were kept constant during the simulation using the SHAKE algorithm,[37] as were the bond angles of the water molecules.

In the gas-phase simulation, the initial internal coordinates of the chain such as the bond lengths, the bond angles, and the dihedral angles were taken from the MP2 gradient ab initio

(29) (a) Müller-Plathe, F.; van Gunsteren, W. F. *Macromolecules* **1994**, *27*, 6040. (b) Smith, G. D.; Jaffe, R. L.; Yoon, D. Y. *J. Phys. Chem.* **1993**, *97*, 12752.

(30) Tasaki, K. *Polym. Prep.* **1994**, *35*, 763.

(31) Jaffe, R. L.; Smith, G. D.; Yoon, D. Y. *J. Phys. Chem.* **1993**, *97*, 12745.

(32) The torsional potential was described by $(1/2)k_\phi[\cos n(\phi - \phi_0)]$ with $1 \le n \le 3$ in ref 29b.

(33) (a) Jorgensen, W. L. *J. Am. Chem. Soc.* **1981**, *103*, 335. (b) Jorgensen, W. L.; Ibrahim, M. *J. Am. Chem. Soc.* **1981**, *103*, 3976.

(34) For POE with more than ten EO units, the physical properties such as the chemical shift and the spin−lattice NMR relaxation time of the methylene protons have been found to be independent of molecular weight.[35]

(35) (a) Liu, K.-J. *Macromolecules* **1968**, *1*, 213. (b) Liu, K.-J.; Ullman, R. *J. Chem. Phys.* **1968**, *48*, 1158.

(36) Verlet, L. *Phys. Rev.* **1967**, *159*, 98.

(37) Van Gunsteren, W. F.; Berendsen, H. J. C. *Mol. Phys.* **1977**, *34*, 1311.

calculations of 1,2-DME.[30] After 20 ps of equilibration at 300 K, the simulation was continued for 5 ns.

In the aqueous-solution simulation, the collapsed chain obtained from the end of the gas-phase simulation was superimposed on the coordinates of a well-equilibrated cubic box of 945 water molecules. Those water molecules which overlapped any of the POE atoms were eliminated from the system, leaving 941 water molecules and one solute in the system. Then the box length was set to 30.83 Å to yield the density of 1.001 g $cm^{-3}$ for the POE aqueous solution at room temperature and 1 atm.[38] The concentration of this resulting solution was 0.058 M. The cubic water box was subject to minimum image periodic boundary conditions[39] to eliminate edge effects.

The effect of various long-range interaction cutoff schemes on pure water has been previously investigated.[40] It was found that the cutoff of 8 Å with the switching function[41] based on the group-by-group truncation yielded reasonable structural and dynamical characteristics of pure water when the SPC water model[42] was used. We have thus chosen the same water model and the same treatment for long-range nonbonded interactions. A number of biomolecule simulations in condensed phase have demonstrated that treatment of electrostatic interactions with an 8-Å cutoff and use of the switching function does not lead to a serious distortion of the structure for a neutral system.[19,43] After minimization to remove any van der Waals contacts between the POE chain and the water molecules, the system was equilibrated for 20 ps during which atomic velocities were either scaled or assigned if the temperature deviated by ±5 K from 300 K. After the equilibration, the simulation was continued for another 2 ns for data collection. No large fluctuations in either the temperature or the total energy were observed, and the total energy was adequately conserved throughout the simulation: the ratio of the root-mean-square fluctuation of the total energy over that of the kinetic energy was maintained within 0.001. During the simulation, the coordinates were saved at every tenth time step for subsequent analysis. A 2-ns simulation for this system of 2937 atoms required 45 days of CPU time on a Silicon Graphics Power Challenge, using one R8000 processor.

## Results and Discussion

**Conformation of POE in Water.** The POE chain in the gas phase quickly transformed from an all-trans extended conformation to a collapsed chain in the first 10 ps of the equilibration period. Similar observations have been made for the same polymer as well as other polymers in the gas-phase simulations.[44] A snapshot taken from the end of the five nanosecond simulation is shown as a chain at the beginning (0 ps) of the solution simulation in Figure 1.

Figure 1 illustrates snapshots of the POE chain at various stages of the simulation in water: at 0, 100, 500, 1000, 1500, and 2000 ps. A coiled conformation obtained from the end of the gas-phase simulation became a helical conformation after 500 ps, and it was maintained at least until 2 ns with some fluctuations mainly along the helical axis. There are strong evidences from Raman[3c] and infrared spectroscopic studies[5b] that POE forms a helix in aqueous solutions. The helical conformation of POE was maintained by the OC−CO sequences exclusively gauche except for the terminal EO units and by the CO−CC sequences mainly trans, also in good accord with experiments.[4,5c]

The average total gauche (gauche$^+$ and gauche$^-$) populations for the C−C and the C−O bonds are 1.0 ($p_{G^+} = 0.33$ and $p_{G^-} = 0.67$) and 0.06 ($p_{g^+} = 0.02$ and $p_{g^-} = 0.04$),[45] respectively, in good agreement with the NMR study, 0.9 and 0.1, respectively.[4] The average torsion angles are $\langle\phi_{G^+}\rangle = 63.7°$ and $\langle\phi_{G^-}\rangle = 291.7°$ for the C−C gauche$^+$ and gauche$^-$ conformations,[45] respectively, and $\langle\phi_t\rangle = 189.0°$, $\langle\phi_{g^+}\rangle = 98.5°$, and $\langle\phi_{g^-}\rangle = 262.6°$ for the C−O trans, gauche$^+$, and gauche$^-$ conformations, respectively. We must note that these values are nonequilibrated characteristics. We later compare these numbers with those obtained after changing the solvent back to water and also after a simulated annealing at 1000 K. In the gas phase, on the other hand, these values were shifted to $\langle\phi_T\rangle = 180.8°$, $\langle\phi_{G^+}\rangle = 68.34°$, $\langle\phi_{G^-}\rangle = 292.1°$, $\langle\phi_t\rangle = 179.8°$, $\langle\phi_{g^+}\rangle = 83.2°$, and $\langle\phi_{g^-}\rangle = 276.7°$.[45] A larger solvation effect is observed on the C−O bond torsion angles than on the C−C bond torsion angles, consistent with the greater flexibility of the C−O bond rotation observed above.

The conformation of POE did not reach its equilibrium for 2 ns. The relaxation time for the bond rotation of POE in water turned out to be extremely long, and the internal bonds, particularly the C−C bonds, of the POE chain underwent only a few conformational transitions (<5). Thus, the helix may not be the most stable conformation of POE in water. To identify the most stable conformation requires a much longer simulation, ∼10 ns or more, which is not practical with a conventional workstation, or an alternative technique has to be taken such as umbrella sampling.

Here, we only examine the stability of the POE helix by two additional simulations: a simulation in a different solvent and a simulated annealing. The conformation of POE is known to be sensitive to the solvent.[5] First, we changed a solvent from water to benzene and observed the conformational change. The simulation was performed for the same POE chain in a cubic box of 191 benzene molecules subject to periodic boundary conditions. The box length of 30.32 Å yielded the density of 0.881 g $cm^{-3}$ for the POE benzene solution at room temperature. The detail of the simulation is found elsewhere.[46] The helix taken from the end of the 2-ns simulation in water was quickly transformed to a coil conformation in the first 200 ps and stayed in a coil for 5 ns. This observation is consistent with several experimental reports.[1,47]

It is of interest to switch the solvent back to water to examine the uniqueness of the POE helix in water. The POE coil taken from the end of the 5-ns simulation in a benzene solution was immersed in a cubic box of 945 water molecules in the same way described above, and a simulation was performed for 1 ns. The adjusted box length was 30.73 Å and the concentration was 0.058 M. Figure 2 shows the snapshots of the POE chain in going from aqueous solution (top) to benzene solution (middle) and from benzene solution back to aqueous solution

(38) The density $d$ was assumed to be $d = x_{POE}d_{POE} + x_{H2O}d_{H2O}$ where $x_{POE}$ and $x_{H2O}$ are the mole fractions of POE and water in the system used, respectively, and the densities $d_{POE} = 1.128$ g $cm^{-3}$ and $d_{H_2O} = 1.00$ g $cm^{-3}$ at 298 K.

(39) Metropolis, N.; Rosenbluth, A. W.; Rosenbluth, M. N.; Teller, A. H.; Teller, E. *J. Chem. Phys.* **1953**, *21*, 1087.

(40) Tasaki, K.; McDonald, S.; Brady, J. W. *J. Comp. Chem.* **1993**, *14*, 278.

(41) Stillinger, F. H.; Rahman, A. *J. Chem. Phys.* **1974**, *60*, 1545.

(42) Berendsen, H. J. C.; Postma, J. P. M.; van Gunstren, W. F.; Hermans, J. In *Intermolecular Forces*; Pullman, B., Ed.; Reidel: Dordrecht, 1981; p 331.

(43) (a) van Gunsteren, W. F.; Karplus, M. *Biochemistry* **1982**, *21*, 2259. (b) van Gunsteren, W. F.; Berendsen, H. J. C.; Hermans, J.; Hol, W. G. J.; Postma, J. P. M. *Proc. Natl. Acad. Sci. U.S.A.* **1983**, *80*, 4315. (c) Wong, C. F.; McCammon, J. A. *Isr. J. Chem.* **1986**, *27*, 211. Levitt, M. *Chem. Scr.* **1989**, *29A*, 197.

(44) Tanaka, G.; Mattice, W. L. *Macromolecules* **1995**, *28*, 1049.

(45) The upper (T/G) and lower (t/g) cases refer to the C−C (trans/gauche) and C−O (trans/gauche) bond conformations, respectively.

(46) Tasaki, K. *Macromolecules*. Submitted for publication.

(47) Liu, K.-J.; Parsons, J. L. *Macromolecules* **1969**, *2*, 529.

(48) Takahashi, Y.; Tadokoro, H. *Macromolecules* **1973**, *6*, 672.

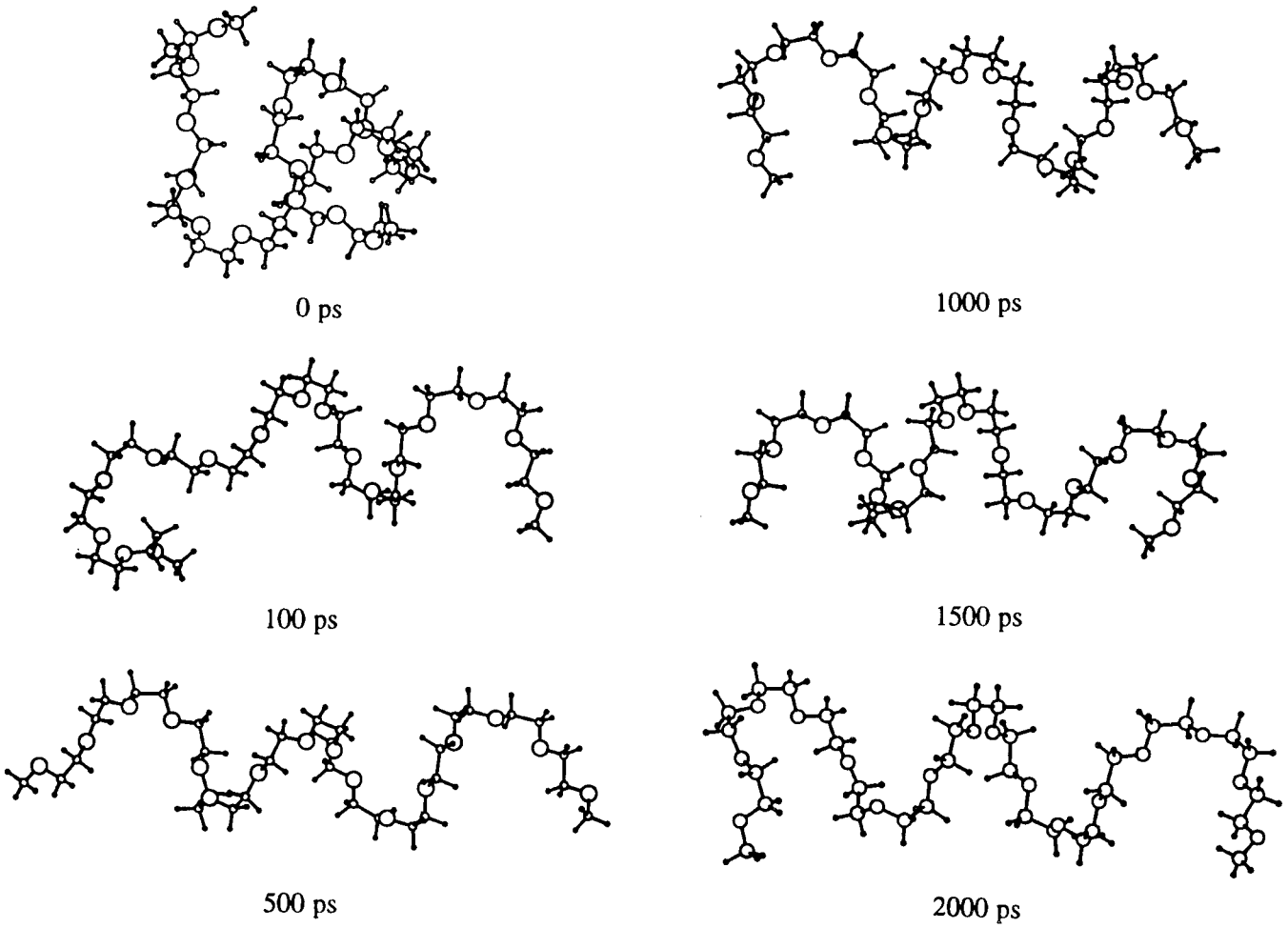


**Figure 1.** Snapshots of the POE chain at the beginning, 0 ps, of the simulation (or at the end of the gas-phase simulation) and at 100, 500, 1000, 1500, and 2000 ps in water. Water molecules are not shown. The chains are placed so that the chain axes are on the figure plane.

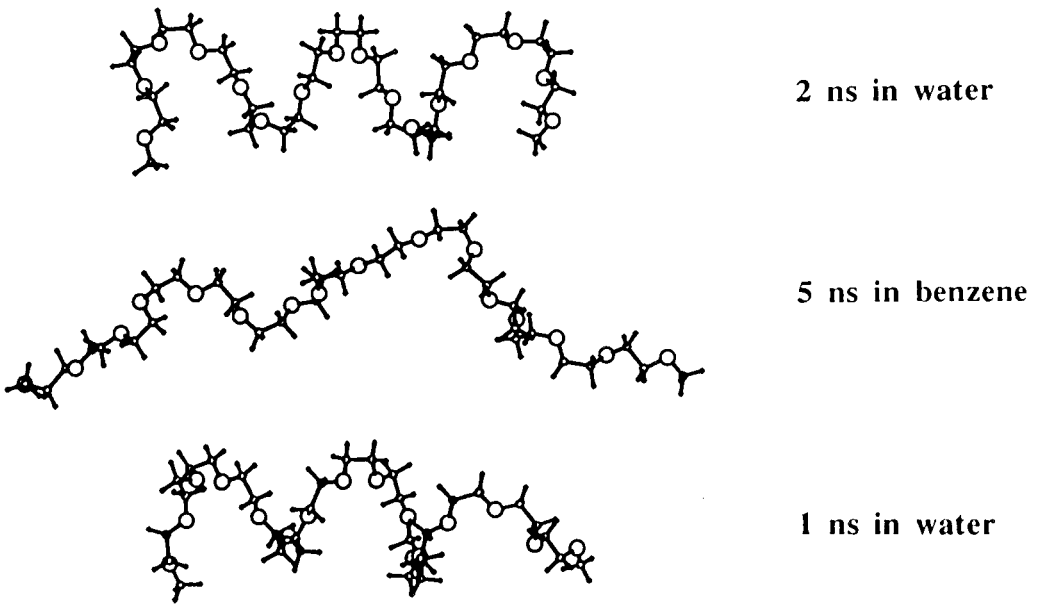


**Figure 2.** Snapshots of the POE chain in a series of simulations in water first, then in benzene, and back to water: at the end of the 2-ns simulation in water (top), the end of the subsequent 5-ns simulation in benzene (middle), and the end of the following 1 ns simulation in water (bottom). See the text for detail.

(bottom). The coil conformation in a benzene solution was transformed to a helix in water again in the first 500 ps and stayed for another 500 ps in water. This helix had similar conformational characteristics as those originally observed in water. The average conformational populations for this helix are $p_{G^+} = 0.42$, $p_{G^-} = 0.58$, $p_{g^+} = 0.02$, and $p_{g^-} = 0.05$. The average torsion angles are $\langle\phi_{G^+}\rangle = 70.4°$, $\langle\phi_{G^-}\rangle = 293.2°$, $\langle\phi_t\rangle = 181.7°$, $\langle\phi_{g^+}\rangle = 115.1°$, and $\langle\phi_{g^-}\rangle = 271.5°$.

Secondly, in the simulated annealing, the system taken from the end of the 2-ns simulation was heated at the rate of 10 K/ps from 300 to 1000 K in the same aqueous solution. The system was equilibrated for 100 ps at 1000 K and then gradually cooled

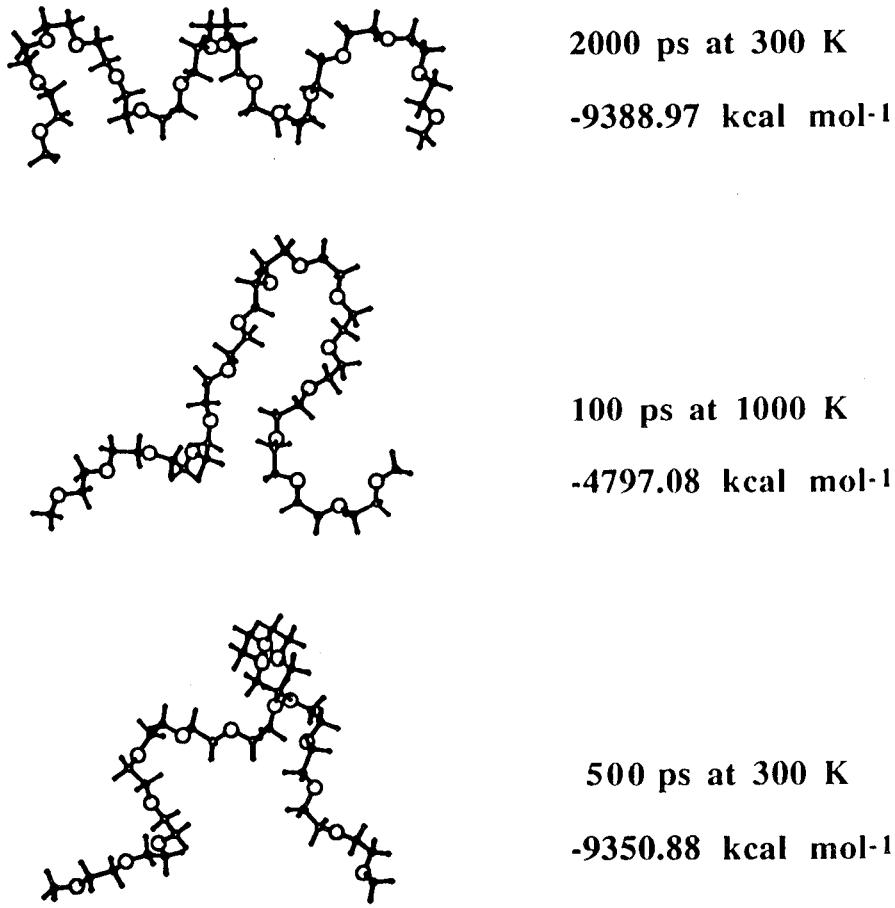


**Figure 3.** Snapshots of the POE chain in the simulated annealing: at the end of the 2-ns simulation at 300 K (top), the end of the subsequent 100-ps simulation at 1000 K (middle), and the end of the following 500-ps simulation at 300 K (bottom) along with the total potential energy of the system. See the text for detail.

down to 300 K at the same rate as that for the heating, followed by 100 ps of equilibration. Subsequently, a simulation was performed for 500 ps at 300 K. Figure 3 illustrates snapshots of the POE chain at three stages of the simulated annealing along with the potential energy of the system at each temperature. The rms flucutation of the potential energy was around 30 kcal $mol^{-1}$ at 300 K. The helix was completely broken at 1000 K, the chain behaving as a disordered random coil. After the system was cooled, the POE chain apparently assumed a helix again at 300 K in 200 ps, as is shown in Figure 3. The helix is bent at the center, consisting of two parts with two different helical senses. During the transformation from a coil to a helix in the cooling, the thermal energy at high temperatures probably provided enough energy to overcome the activation energy for the helix to switch the helical sense at the center which led to a bending of the helix. The bent helix shown in Figure 3 was maintained at least for 500 ps. For comparison to the helix before the simulated annealing, the conformational populations are $p_{G^+} = 0.40$, $p_{G^-} = 0.60$, and $p_{g^\pm} = 0.01$ for one helix and $p_{G^+} = 0.86$, $p_{G^-} = 0.14$, and $p_{g^\pm} = 0.00$ for another. The average torsion angles are $\langle\phi_{G^+}\rangle = 62.61°$, $\langle\phi_{G^-}\rangle = 292.95°$, $\langle\phi_t\rangle = 179.43°$, $\langle\phi_{g^+}\rangle = 100.12°$, and $\langle\phi_{g^-}\rangle = 257.73°$ for one helix and $\langle\phi_{G^+}\rangle = 70.20°$, $\langle\phi_{G^-}\rangle = 295.16°$, and $\langle\phi_t\rangle = 81.71°$ for another. One of the helices is more stretched than the other. More detailed analysis of the helices will be reported in a forthcoming paper. The above two simulations support the uniqueness of the POE helix in an aqueous solution. Nevertheless, further study is warranted for the most stable conformation of POE in water.

To examine the conformation of POE in the context of the water structure, the pair distribution function (PDF) for the POE oxygen atoms was calculated. The PDF is defined as[18a]

$$g(r) = (1/4\pi\rho r^2)\, \mathrm{d}N(r)/\mathrm{d}r \qquad (2)$$

where $\rho$ is the POE ether oxygen atom number density, $r$ the interatomic distance between two POE oxygen atoms in question, and $N$ the number of oxygen atoms within the distance $r$. Figure 4 displays the POE oxygen−oxygen PDF, along with the bulk water oxygen−oxygen PDF. The bulk water molecules are defined as water molecules separated from the POE oxygen atoms by more than 3.5 Å and from the methylene carbon atoms by more than 4.5 Å.[19a] The figure shows that the peak positions for the POE oxygen atoms coincide well with those for the bulk water oxygen atoms. The first peak around 2.85 Å arises from the nearest POE oxygen atoms in the gauche conformation around the C−C bond, and the second peak around 4.8 Å from the oxygen atoms in the nearest adjacent EO unit in the $-[tG^{\pm}t]_i[tG^{\mp}t]_{i+1}-$ conformation. The shoulder of the second peak around 5.2 Å is due to the ether oxygens also in the nearest adjacent EO unit but in a different C−C conformational sequence, i.e., the $-[tG^{\pm}t]_i[tG^{\pm}t]_{i+1}-$ conformation. Likewise, the third peak around 6.35 Å is assigned to the ether oxygens in the second nearest adjacent EO units.

Table 2 lists the characteristics of the PDF for the POE ether oxygen atoms in comparison to those for the bulk water oxygen atoms. The agreement in the PDF peak positions between the POE oxygen and the bulk water is consistent with Blandamar and co-workers's model[12] that a POE chain assumes the gauche conformation around the C−C bond which least disturbs the water structure. However, their model does not necessarily lead to a helix structure since they only discuss the closest O···O distance in the gauche conformation around the C−C bond. Our results, on the other hand, are consistent with the preference of a helix as a favorable chain conformation in water. With the

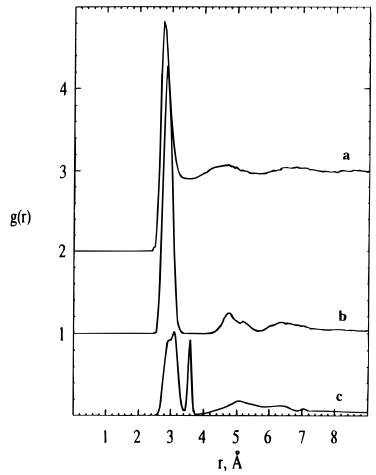


**Figure 4.** Pair distribution functions for (a) the bulk water oxygen atoms, (b) the POE helix oxygen atoms in water, and (c) the POE coil oxygen atoms in benzene.

helical conformation, each ether oxygen atom can replace a water oxygen atom with the minimum structural perturbation to water. Thus, the helical structure of POE can be accommodated into the hexagonal water structure without much perturbation.

The succession of the $-[tG^{\pm}t]_i[tG^{\mp}t]_{i+1}-$ conformation leads to an overlap of the chain with itself. Therefore, in order to avoid the overlap, the POE chain generates some fractions of the $-[tG^{\pm}t]_i[tG^{\pm}t]_{i+1}-$ conformation which gave rise to the shoulder peak around 5.2 Å. Other thermodynamic factors are certainly in effect, stabilizing the helix such as a strong hydration by water, as is discussed later. Nevertheless, the structural fitness of the helix to water seems an important element in understanding the stability of the helix and the unique solubility of POE in water.

Figure 4 also displays the PDF for a random coil POE chain obtained from the above benzene-solution simulation. It is well-illustrated in the disagreement of its peak positions with those for the bulk water that a random coil disrupts the water structure, thus an unfavorable chain conformation in water. It is worth noting that the C−C and C−O bonds of the POE coil still favor the gauche and trans conformations, respectively, in a benzene solution.

Some experimental evidence suggests that a POE chain in water retains a helical conformation observed in the crystal.[5b,c] To characterize the helical structure of POE in water, we analyzed the number of the repeating units in one helical turn. It was found that the POE chain had roughly a (11/2) helix with the average helical pitch of about 16 ± 3 Å, although this characterization is not as clearly defined as that in crystal due to the constant stretching movement along the helix and the flexibility of the chain. On the other hand, the crystal POE has a (7/2) helix with a helical pitch of 19.48 Å.[48] Though a direct comparison is difficult, the POE chain in water seems to have at least a more compressed helix with a larger diameter, around 5 Å, than that of the crystal POE. The larger diameter enables the helix to accommodate some water molecules inside. This is a consequence of the helix in which the ether oxygen atoms point inward and the methylene carbon atoms outward; thus water molecules enter into the helix for more favorable hydration. The compression of the helix arises from the existence of the $-[tG^{\pm}t]_i[tG^{\mp}t]_{i+1}-$ conformation in POE in water. This is due to the increased flexibility of the POE chain in going from the crystal to water, which has been suggested by an infrared spectroscopic study.[5b] The POE chain observed in water after the simulation in benzene, shown in the bottom of Figure 3, also had a (11/2) helix with a pitch of 17 ± 3 Å.

In crystal, the conformation of POE is found to be either all gauche$^+$ or all-gauche$^-$ around the C−C bond.[48] This helical conformation yields a second peak in the oxygen−oxygen PDF around 5.3 Å instead of 4.8 Å. Since the bulk water oxygen PDF does not have a peak around 5.3 Å, the helical conformation found in the crystal would not fit in the hexagonal water structure as nicely as the helical conformation observed in our MD simulations.

**Hydration Structure.** Figure 5 illustrates a snapshot of a typical hydration structure including a part of the POE chain with only some relevant water molecules inside the helix, taken from the dynamics trajectory. It was found that most of the water molecules inside the helix were trapped throughout the simulation. An average residence time for individual water molecules to stay near their closest POE oxygen atoms (when a water oxygen is within 3.5 Å from a POE oxygen) was approximately 25 ps, and the cumulative residence time was about half the entire simulation. Thus, the hydration structure illustrated in Figure 5 represents a significant part of the 2-ns simulation. We observed that water molecules inside the helix form an extensive network of hydrogen bonds with POE and with themselves, stabilizing the helical backbone.

There seems to be at least two types of water molecules inside the helix in the way they form hydrogen bonds with POE. There are the water molecules (*a* and *b*) bridging two POE oxygen atoms separated by two EO units and those (*c* and *d*) bridging a POE oxygen atom on one hand and a water molecule on the other which is bridged to a different POE oxygen. While the latter hydrogen-bond coordination has been proposed by Luck,[15b] the former is a new bridged structure found in this study. Similar hydrogen-bond structures have been found in other systems such as papain where one-molecule or two-molecule water bridges hydrogen bonded to a solute.[49] The stabilizing effect of water molecules specifically hydrogen bonded to different residues on structures of biopolymers has also been reported.[50]

Figure 6 illustrates the PDF for the POE oxygen atom and the nearby water oxygen atoms. The result for Figure 6 was averaged over all the POE ether oxygens except the terminal EO units. The sharp, narrow first peak indicates strong specific interactions with the nearby water molecules, i.e., a hydrogen bond, a characteristic similar to the bulk water oxygen PDF except for the peak's height (see Figure 5). Markedly strong structuring effects on the water molecules nearest neighbor to the POE oxygen are observed in the PDF. The second peak at 4.45 Å is significantly high in sharp contrast to that of the bulk water PDF shown in Figure 4. This is well-illustrated in Figure 5. A high probability of finding water b, about 4.4 Å apart from the ether oxygen α, strongly associated with the other ether oxygen atoms $\gamma$ and $\theta$ simply increases the second peak height of the ether oxygen α's PDF.

The characteristics of the POE oxygen−water oxygen PDF are listed in Table 2. Our MD simulation yielded 2.91 water molecules associated with an EO unit of POE obtained from integrating the distribution curve (Figure 6) out to the first minimum at 3.35 Å. This number is in excellent agreement with the recent differential scanning calorimetry study[16] which reported 2.6 water molecules per EO unit.

(49) Drenth, J.; Jasonius, J. N.; Koekoek, R.; Wolthers, B. G. *Adv. Protein Chem.* **1971**, *25*, 79.

(50) Berendsen, H. J. C. In *Water: A Comprehensive Treatise*; Franks, F., Ed.; Plenum: New York, 1975; Vol. 5, p 293.

(51) (a) Hecht, D.; Tadesse, L.; Walters, L. *J. Am. Chem. Soc.* **1992**, *114*, 4336 and references therein. (b) Maeda, Y.; Tsukida, N.; Kitano, H.; Terada, T.; Yamakawa, J. *J. Phys. Chem.* **1993**, *97*, 13903.

**Table 2.** Characteristics of the Pair Distribution Functions for POE Oxygen and Water Oxygen Atoms

| | At 300 K | | | | |
|---|---|---|---|---|---|
| | $O_{POE}\cdots O_{POE}$[a] | $O_{POE}\cdots O_{H_2O}$[b] | $O_{H_2O}\cdots O_{H_2O}$[c] | $O_{H_2O}\cdots O_{H_2O}$[d] | $O_{H_2O}\cdots O_{H_2O}$[e] |
| first maximum, Å | 2.85 | 2.75 | 2.75 | 2.75 | 2.75 |
| height | 3.28 | 1.95 | 2.58 | 3.18 | 2.83 |
| first minimum, Å | | 3.35 | 4.30 | 3.90 | 3.55 |
| second maximum, Å | 4.80 | 4.45 | | | 4.75 |
| height | 0.25 | 1.43 | | | 1.07 |
| shoulder in second peak, Å | 5.20 | | | | |
| second minimum, Å | | 6.20 | | | 5.65 |
| third maximum, Å | 6.35 | 7.15 | 6.80 | 6.50 | 6.50 |
| height | 0.14 | 0.99 | 1.24 | 1.17 | 1.05 |
| water molecules within 3.4 Å | 2.0 | 2.91 | 4.71 | 5.71 | 4.77 |

| | At 373 K | | | |
|---|---|---|---|---|
| | $O_{POE}\cdots O_{H_2O}$[b] | $O_{H_2O}\cdots O_{H_2O}$[c] | $O_{H_2O}\cdots O_{H_2O}$[d] | $O_{H_2O}\cdots O_{H_2O}$[e] |
| first maximum, Å | 2.75 | 2.80 | 2.80 | 2.80 |
| height | 1.76 | 2.41 | 2.80 | 2.45 |
| first minimum, Å | 3.35 | 4.25 | 4.00 | 3.90 |
| second maximum, Å | 4.40 | | | 4.60 |
| height | 1.39 | | | 1.04 |
| shoulder in second peak, Å | | | | |
| second minimum, Å | 6.25 | | | |
| third maximum, Å | 7.30 | 6.55 | 6.65 | |
| height | 1.06 | 1.18 | 1.08 | |
| water molecules within 3.4 Å | 3.23 | 5.33 | 5.81 | 4.89 |

[a] The POE oxygen−oxygen PDF. [b] The POE oxygen−water oxygen PDF. [c] The water oxygen−oxygen PDF near the POE oxygen atom. [d] The water oxygen−oxygen PDF near the POE methylene carbon atom. [e] The bulk water oxygen−oxygen PDF.

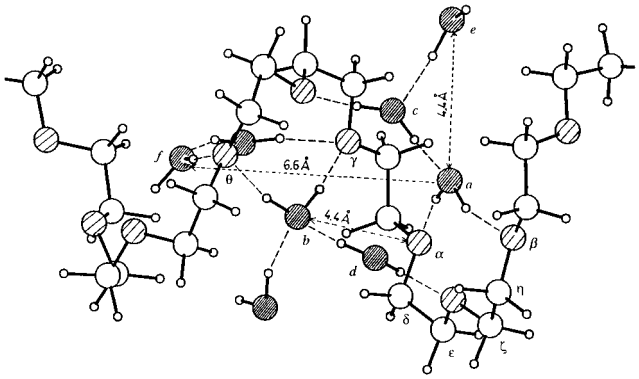


**Figure 5.** Snapshot of a part of the POE chain with some water molecules inside the helix taken from the dynamics trajectory. Other water molecules are removed for clarity. The water oxygens are densely hatched, while the ether oxygens are lightly hatched.

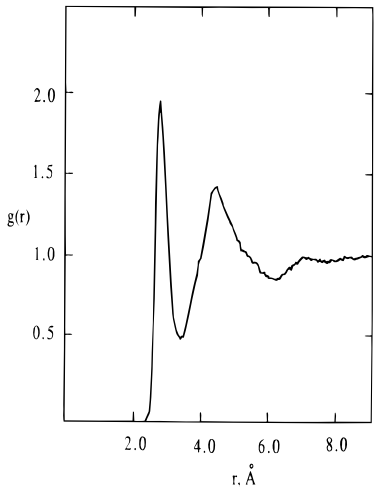


**Figure 6.** POE ether oxygen−water oxygen pair distribution function. The result was averaged over all the POE oxygen atoms except for the terminal EO units.

Figure 7 displays the normalized orientational distribution function $P(\cos(\theta))$ for the water molecules near the POE oxygen averaged over several ether oxygens around the center of the chain. This function is the probability of finding an angle $\theta$ between each of the O−H bond vectors in the nearest-neighbor water molecules and the vector defined by the line from the POE oxygen to the water oxygen. In the calculations of the distribution function, the nearest-neighbor distance is defined as the distance of the first minimum in the PDF (3.35 Å from the ether oxygen).[19a] All water molecules within this cutoff distance were included in the averaging. The function was normalized such that the integration of the curve is the total number of water molecules within 3.5 Å from a POE oxygen atom, 2.9. The behavior of the distribution curve shown in Figure 7 is typical of hydrogen bonding.[19a,20a] The strong peak at −1 indicates one of the hydrogens of nearest-neighbor water molecules pointing directly at the ether oxygen. The broad secondary peak around +0.4 is a consequence of the tetrahedral structure of the rigid SPC water molecules.[42] The hydrogen bonds between POE and water molecules inside the helix were maintained without breakup for a significant part of the simulation. On the other hand, spontaneous breakups were frequently observed for the hydrogen bonds between the terminal EO unit and nearby water molecules.

**Water Structure and Dynamics.** Figure 8 demonstrates the oxygen−oxygen PDF for the water molecules near the POE ether oxygen. In the calculation, the water molecule spending the longest time near a POE oxygen atom was first identified from the trajectory. The average total time of such water molecules being near the POE oxygen atom was approximately 250 ps out of 500 ps for which the data were analyzed. Then, the PDF was calculated as a probability of finding other water molecules within the distance $r$ from the water molecule nearest neighbor to the POE oxygen atom. The distribution curve was averaged over the water molecules near several POE oxygen atoms around the center of the chain. Since this is a water oxygen−oxygen PDF, it can be directly compared to that for the bulk water to analyze the water's structural characteristics near the POE oxygen. The PDF for the bulk water is also shown in the same figure.

A significant enhancement in the water structure around the POE oxygen is demonstrated which is in line with the above

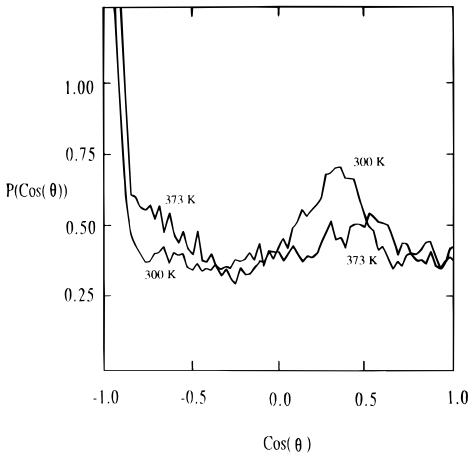


**Figure 7.** Normalized orientational distribution function $P(\cos(\theta))$ for the water molecules near the POE ether oxygen atom, averaged for several central ether oxygens of POE at 300 and 373 K.

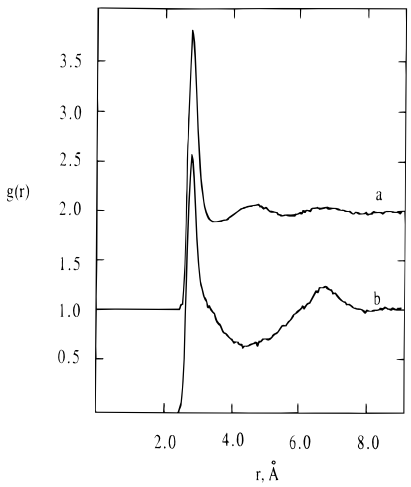


**Figure 8.** Water oxygen−oxygen pair distribution function: (a) the bulk water and (b) the water molecules near the POE oxygen. The result was averaged over several POE oxygen atoms around the center of the chain.

POE oxygen−water oxygen PDF. The remarkable contrast to the bulk water is the absence of the second peak and the much larger third peak in the PDF for the nearby water oxygens. These characteristics of the PDF are consistent with the hydration structure shown in Figure 5. Namely, the water molecule a bridging the POE oxygen atoms α and $\beta$ can have nearby water molecules such as c or e only in the opposite side of α and $\beta$. Thus, the water molecule a has a smaller number of nearby water molecules around 4.75 Å due to the presence of α and $\beta$ and also to a small water accessibility of the hydrophobic methylene groups $\delta$, $\epsilon$, $\zeta$, and $\eta$. This gives rise to the absence of the second peak in Figure 8. The contribution to the high third peak is the increased probability of finding other water molecules such as f, hydrogen bonded to the ether oxygen $\theta$, around 6.6 Å apart from a, three EO units away from the ether oxygen α.

Figure 9 displays the oxygen−oxygen PDF of the water molecules near the POE methylene carbon averaged over several central EO units. Since the water molecules within 3 Å from the methylene carbon can be hydrogen bonded to the adjacent ether oxygen, only the water molecules closer to the methylene carbon than to the adjacent POE oxygen atoms were selected. This is to examine the effect of the methylene carbon atom on the nearby water structure rather than the effect of the POE oxygen atom. The average total time of the water molecule being near the methylene carbon was approximately 40 ps out

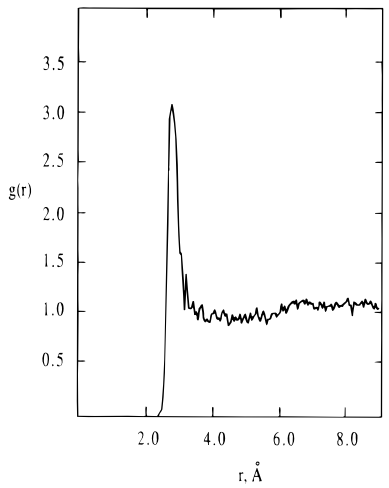


**Figure 9.** Oxygen−oxygen pair distribution functions for the water molecules near the POE methylene carbon atom averaged over several central EO units.

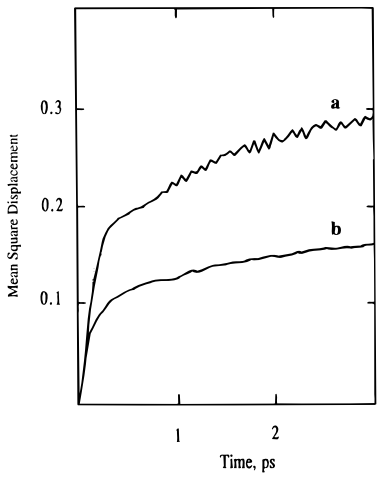


**Figure 10.** Mean-square displacements of water molecules: (a) water molecules near the POE methylene carbon and (b) those near the POE ether oxygen. The values were averaged over several central EO units.

**Table 3.** Translational Diffusion Coefficients for Water Molecules Near the POE Oxygen Atom and the Methylene Carbon Atom ($\times 10^{-5}$ cm$^2$ s$^{-1}$)

| temp (K) | ether oxygen | methylene carbon | bulk |
|---|---|---|---|
| 300 | 0.02 | 0.04 | 3.3 |
| 373 | 0.05 | 0.28 | 11.3 |

of 500 ps, significantly shorter than that for the water molecule near a POE oxygen. The average residence time of a water molecule around the methyl group (when a water oxygen is within 4.5 Å from the methylene carbon and more than 3.5 Å from the adjacent POE oxygen) was 12 ps. The number of water molecules integrated out to 3.4 Å is 5.71, larger than that for the bulk water, 4.77. In fact, Raman studies report more hydrogen bonds between water molecules in hydrophobic shells.[51]

Figure 10 displays the center-of-mass mean-square displacements of the water molecules near POE. Curve a corresponds to the water molecules within 4.5 Å from the methylene carbon, and curve b to those within 3.5 Å from the ether oxygen atom. The values were averaged over several central EO units. Due to the short time spent by the water molecule near the methylene carbon atom, as is described above, more noise is observed for those water molecules (curve a). Table 3 lists their translational diffusion coefficients including the bulk water's estimated from a least-squares analysis of the limiting slopes of the curves in Figure 10. An extremely low diffusion coefficient for the water

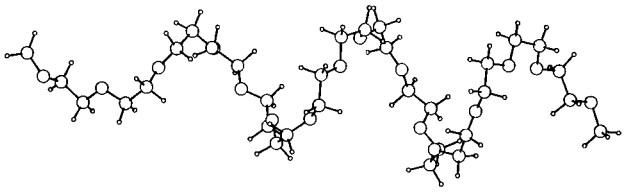

**Figure 11.** Snapshot of the POE chain taken from the end of the 1-ns simulation at 373 K. Water molecules are not shown.

molecules adjacent to the ether oxygens, and those near the methylene carbon to a lesser extent, is observed, compared to the bulk water. The slow diffusion of the water molecules near the methylene carbon atom is apparently influenced by the nearby ether oxygen due to its proximity. It is, however, difficult to estimate the extent to which the water molecules near the methylene carbon atom are affected by the nearby ether oxygen. In any case, the results indicate a significant reduction in the translational freedom of the water molecules near POE. This is well-illustrated by a snapshot shown in Figure 5. The water molecules inside the helix tightly bridge between the ether oxygens or between the ether oxygen and the nearby water molecules, building a rigid hydrogen-bond network through the inside of the helix. The dynamics trajectory indicated that those water molecules spent most of the time inside the helix almost throughout the simulation. A considerably slow decay of the reorientation autocorrelation function for the water molecules confined inside 18-crown-6 also has been reported.[52] Quasielastic neutron scattering measurements[17] of POE in aqueous solution report the water structure near POE which is consistent with our finding.

**Conformation and Hydration of POE at 373 K.** Bailey and Callard interpreted the phase separation of POE at a cloud point in terms of a hydrophilic−hydrophobic balance in the polymer structure and also in terms of the increase in the activity of the neutral polymer molecule with increasing temperature.[6a] Here, we examine the conformation and the water structure of the POE chain at 373 K, a cloud point of POE. Starting from the end of the 2-ns simulation, an additional MD simulation of the same system was performed by raising the temperature at the rate of 9 K/ps from 300 to 373 K. The system was equilibrated for 20 ps at 373 K and subjected to simulation for 1 ns from which the data were collected for analysis. The average end-to-end distance has increased somewhat to 25.42 Å from 21.95 Å at 300 K. This increase is attributed to a small conformational change. Figure 11 illustrates a snapshot of the POE chain taken from the end of the 1-ns simulation at 373 K. Basically, the POE chain was still maintained as an (11/2) helix with $17 \pm 4$ Å of the average helical length, somewhat stretched compared to the helix at 300 K. The frequency of the gauche$^{\pm}$ → trans conformational transition around the C−C bonds only near the terminal groups of POE increased at 373 K. A modest degree of the disorder in the conformation was observed mainly due to the increased thermal motion of the chain.

The individual conformational populations for the C−C bond rotation averaged over the chain except for the terminal units were $p_T = 0.00$, $p_{G^+} = 0.33$, and $p_{G^-} = 0.67$ at 300 K and $p_T = 0.00$, $p_{G^+} = 0.27$, and $p_{G^-} = 0.73$ at 373 K. The population of the total gauche$^-$ conformation around the C−C bond has increased by only 0.06 from that at 300 K. The conformational populations for the C−O bond changed even to a lesser extent: $p_t = 0.94$, $p_{g^+} = 0.02$, and $p_{g^-} = 0.04$ at 300 K and $p_t = 0.94$, $p_{g^+} = 0.03$, and $p_{g^-} = 0.03$ at 373 K. The average torsion angles for the gauche$^{\pm}$ conformations around both C−C and C−O bonds show only a minor difference from those at 300 K: $\langle\phi_{G^+}\rangle = 63.42°$, $\langle\phi_{G^-}\rangle = 291.98°$, $\langle\phi_t\rangle = 176.56°$, $\langle\phi_{g^+}\rangle = 93.61°$, and $\langle\phi_{g^-}\rangle = 262.13°$, respectively.

Hence, the increase in the end-to-end distance of POE at 373 K arises from a build-up of a slight shift in the gauche$^-$ population around each C−C bond through the chain and also from the increased population of the trans conformation around the terminal C−C bonds. The increase in the end-to-end distance is 3.47 Å which corresponds to around a 0.2-Å increase per EO unit for this size of POE. Thus, the POE chain is somewhat stretched with more population of gauche$^-$ at 373 K, giving rise to a positive temperature coefficient of the unperturbed molecular dimension which has been observed by thermoelastic measurements of POE.[53] This implies that at higher temperatures, a POE chain becomes a more stretched helix with a smaller diameter and thus having a fewer number of water molecules inside the helix, which leads to an unfavorable hydration. This may be another contribution to the phase separation of POE at higher temperatures.

Nonetheless, the change in the overall conformational populations of the POE chain at 373 K is still small. Therefore, our results so far indicate little to support the model presented by Samii et al.[27] that the conformational change with increasing temperature causes unfavorable dipole−dipole interactions between POE and water, leading to a phase separation. To cause unfavorable dipole−dipole interactions at 373 K, POE must have more fractions of trans around the C−C bond since the largest change in dipole−dipole interactions occurs from gauche$^{\pm}$ → trans conformational transitions. However, longer simulations are required to confirm our observation on the conformation at 373 K.

The dynamics trajectory at 373 K also indicated primarily the same hydration structure as that at 300 K. Thus, the hydrogen-bond network inside the helix at 373 K is almost intact, indicating its resilience at the higher temperature at least for 1 ns. If POE assumes a helix even at 373 K, as our simulation indicated, the high helical persistence may be related to POE's pseudoplastic rheological behavior in aqueous dilute solutions.[6g]

The POE oxygen−water oxygen PDF and the water oxygen PDF's near the POE oxygen and methylene carbon were also examined at 373 K. It was found that all the PDF's were basically the same as those at 300 K, indicating that the enhanced water structure near POE remains even at 373 K. Only small changes in the peak heights and the minimum heights were observed due to the increased thermal motion. The characteristics of all PDF's calculated at 373 K are listed in Table 2.

The mean-square translational displacements were calculated for the water molecules near POE in the same manner as the previous section. The results showed somewhat enhanced translational freedoms for the nearby water molecules due to the increased thermal motion. Nevertheless, a least-mean-square fitting to the mean-square translational displacement curves yielded again small values of the self-diffusion coefficient for those water molecules, listed in Table 3, still significantly smaller than that for the bulk water at the same temperature.

The normalized orientational distribution function for the water molecules near the POE oxygen is illustrated in Figure 7 together with that obtained at 300 K. The values between cos-$(\theta) = -1.0$ and 0.0 increased, while those between $\cos(\theta) =$ 0.0 and 0.5 decreased, demonstrating less favorable orientations for the hydrogen bond between POE and water.

The PDF's, the orientational distribution function, and the self-diffusion coefficients of the water molecules near POE all unambiguously demonstrate the enhanced water structure in the

(52) Geiger, A.; Kowall, T. In *Hydrogen Bond Networks*; Bellissent-Funel, M.-C., Dore, J. C., Ed.; Kluwer: Dordrecht, 1994; p 23.

(53) Mark, J. E.; Flory, P. J. *J. Am. Chem. Soc.* **1965**, *87*, 1415.

hydrophilic region, and to a lesser extent the hydrophobic region, and the weakened hydrogen bonds with water at 373 K. These findings suggest that POE precipitates at the cloud point mainly due to the increased unfavorable entropy contribution at a higher temperature, $-T\Delta S$, assuming the same free energy contributions from POE···POE intermolecular interactions at both temperatures. Also, the weakened hydrogen bonds of POE with water at 373 K are to some extent responsible. Therefore, our results support fully the Kjellander's thermodynamics model[11] and partially the Goldstein's hydrogen bond model.[26]

## Conclusions

We have performed a 2-ns MD simulation of POE with 15 EO units in aqueous solution to examine the hydration and the conformation of POE and the water structure and the dynamics near POE. The snapshots from our simulation revealed a rather complex hydration structure of POE in water. The bridged hydrogen bond was observed between POE and water, as has been suggested previously,[15] as well as a new bridged hydrogen bond model found in this study: a water molecule bridged between POE oxygens separated by two EO units. The extensive hydrogen-bond network was found, running through the POE helix, stabilizing the helix. The average number of water molecules associated with each EO unit was 2.9, in excellent agreement with the differential scanning calorimetry,[16] NMR,[5b] and Raman studies,[5d] around 3. However, the number is either considerably smaller than those found by the other NMR study, 5 or 6,[9] or somewhat larger than quasielastic neutron scattering measurements, 1.[17] The detailed hydration structure of POE may help us understand the complex thermodynamics characteristics of POE in water.

The pair distribution functions for the water oxygen atoms in the hydrophilic region of POE, and its hydrophobic region to a lesser extent, strongly indicated the enhanced water structure near POE. Especially, the oxygen−oxygen pair distribution function for the water moelcules near POE oxygens provided the detailed water structure inside the helix, enabling us to gain in-depth understanding of the inside hydration, which could not have been possible with only the POE oxygen−water oxygen pair distribution function. As a result of the enhanced structure, the translational freedom of water near POE was significantly reduced, which is well-illustrated by small self-diffusion coefficients of nearby water. The loss of translational freedom of nearby water leads to a negative entropy of mixing for POE and water over nearly the whole composition range, as has been observed experimentally.[6d,7] We also found the enhanced water structures near POE at 373 K, though they are less significant than those at 300 K. We thus concluded that assuming the same free energy contributions from POE···POE intermolecular interactions at 300 and 373 K, the increased unfavorable entropy contribution, $-T\Delta S$, at the elevated temperature is mainly responsible for a precipitation of POE at the cloud point. The decreased favorable hydration enthalpy contribution due to the weakened hydrogen bonds between POE and water, demonstrated by the orientation distribution of water molecules near POE oxygens, is also ascribed to the precipitation. Both entropic and enthalpic contributions have been suggested by Kejllander and co-workers[11] and Goldstain,[26] respectively.

The conformation of POE was transformed from a collapsed coil to a helix in water, and the helix was maintained for at least 2 ns at 300 K and for 1 ns at an increased temperature, 373 K. It should be emphasized that the simulation was started with a compact coiled chain, not a helix, and there is no parameter in the force field to drive the POE chain to a helix. Our observation is consistent with the previous simulations of POE in water: Depner et al. reported the population of the C−C bond exclusively in gauche,[22a] and Gölander et al.'s simulation showed a helix for the POE conformation.[22c]

Separately, the POE helix obtained from the 2-ns simulation quickly transformed to a random coil-like conformation in a benzene solution. The coiled chain taken from the benzene-solution simulation was again converted to a helix in water. Furthermore, the simulated annealing of the POE chain in water first heated to 1000 K and then cooled down to 300 K still showed a preference for a helix as well, though it was bent at the center with two different helical senses. Our observation so far strongly suggests a helix as a unique conformation of POE in water, although we stress that further study is needed for a more statistically significant validation.

Our model, a POE oligomer chain with 15 repeating units, only represents a part of the polymer chain. Although MD simulations of a longer simulation for a longer POE chain are warranted, we believe that the nature of POE−water interactions found in this study is still relevant, since the simulation is long enough for configurational equilibration of the water molecules in the system used.

Good agreement with experimental results in the conformation and the hydration of POE and the water structure in the vicinity of POE observed in our simulation suggests a validity of the potential energy function and the simulation protocol used. The simulation also provided in detail the information often experimentally difficult to probe. Such information includes the conformational characteristics in water, the local hydration structure, and the structure and the dynamics of water near both the hydrophilic and the hydrophobic shells of POE. The knowledge of these properties greatly enhances our understanding of the solution properties of POE. The same techniques can be applied to other polyethers, not only to understand the difference in the solubility from that of POE but also to comprehend further the nature of water-soluble polymers in general.

**Acknowledgment.** The author is greatly in debt to Prof. J. W. Brady at Cornell University for his helpful comments. All computations were performed in the Chemistry Computing Facility at the Washington University in St. Louis.

JA951005C